

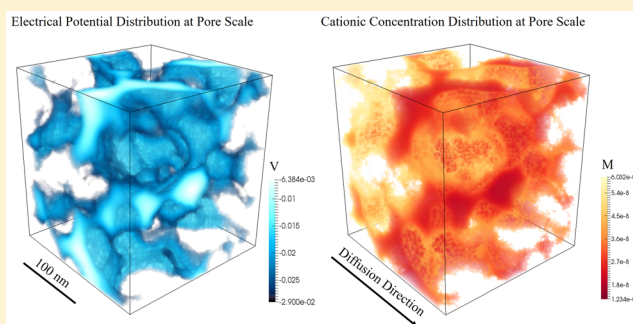
Cation Diffusion in Compacted Clay: A Pore-Scale View

Yuankai Yang and Moran Wang*[✉]

Department of Engineering Mechanics and CNMM, Tsinghua University, Beijing 100084, China

S Supporting Information

ABSTRACT: Cation diffusion through compacted clays is of great interest due to its potential for buffer materials for waste disposal. The importance of the electrokinetic effect on cationic tracer diffusion is investigated by using pore-scale simulations to consider the influence from the electrokinetic properties and topology of clays. It is indicated that the normalized volume charge density has a significant impact on the cationic diffusion. In clays with a large normalized volume charge density, the electrical double layer has the major impact on cationic diffusion. When the ion strength of the pore solution is constant, the flux from the electromigration term can be negligible. However, once an ion strength gradient is added, the electromigration process should be considered carefully due to its non-negligible role to balance the alteration of total flux. The present study could help improve the understanding of the transport mechanism of simple cationic tracers in compacted clays.



1. INTRODUCTION

Due to low permeability, swelling ability, and the large retention capacity for cations, compacted clay-based materials are commonly suggested as the buffer material for the geological disposal of high-level radioactive wastes. Improving the understanding of the mechanism of cation transport through barrier materials is significant to predict the long-term safety. For many cations at low concentrations, it has been reported that the cations diffuse through compacted clay at a greater rate than neutral or negatively charged species.¹ The concept of “surface diffusion” is often employed to explain the large flux of cations compared with neutral species from experimental measurements.² It is usually attributed to the interaction of cations with negatively charged surfaces of clays, and this electrostatic interaction increases the flux along surfaces within the electrical double layer (EDL) referred to the surface diffusion. However, the existence and importance of surface diffusion for different cations in various compacted clays is still doubtful. It was reported that the surface diffusion was unimportant for Cs⁺ in dense clays³ or FEBEX bentonite⁴ and not important for Sr²⁺ and Na⁺ in compacted clays.⁵ Instead, a lot of measurements showed that the surface diffusion was important for Cs⁺ and Na⁺ in compacted montmorillonite¹ or important for Na⁺, Sr²⁺, and Zn²⁺ in compacted illite.^{6,7} Moreover, the importance of surface diffusion through clay-based materials also depends on ion salinity, pH, clay density, and clay composition.^{1,5,6}

Recently, several continuum-scale models have been developed to describe sorbed cation diffusion through compacted clays, such as the models based on the Donnan theory,^{8–11} or the models that may include separated bulk diffusion, surface diffusion, and interlayer diffusion.^{2,12,13}

Admittedly, these phenomenological formulas could enhance the understanding and explain some experimental results, but parameters involved in the generalized Fick’s law had to be determined empirically or by fitting with experiment data. For instance, the surface diffusion coefficient D_s of sorbed cations is often involved in these phenomenological formulas.¹⁴ However, the relative surface diffusion coefficient of the cesium ion depends on the tracer’s concentration ranging from 0.1 to 0.0001² by fitting with the experiment data. Besides, the sorption distribution coefficient K_D is also uncertain. Different methods (batch or diffusion experiment) give various K_D values.¹⁵ To simplify the diffusion in three-dimensional microstructures of clays into the diffusion in a one-dimensional channel, the previous studies^{2,13,16} also assume that the tortuosity of sorbed cations’ diffusion is the same as that of neutral species’ diffusion. This assumption may be reasonable for the interlayer pores in compacted montmorillonite, but for illite or kaolinite without interlayer pores, it may be different due to the rough surfaces of clay particles.¹⁷ In particular, when the pore size is at nanoscale or the clay density is high, the experimental study becomes time-consuming and difficult. Besides, the assumptions and the physical meanings of parameters (e.g., D_s) in the generalized Fick’s law are uncertain for different species and clay minerals. The pore-scale modeling therefore could provide a possible way to contribute to understanding of sorbed-ion transport in compacted clays and to clarify effects from different physical or chemical

Received: October 12, 2018

Revised: January 16, 2019

Accepted: January 17, 2019

Published: January 17, 2019

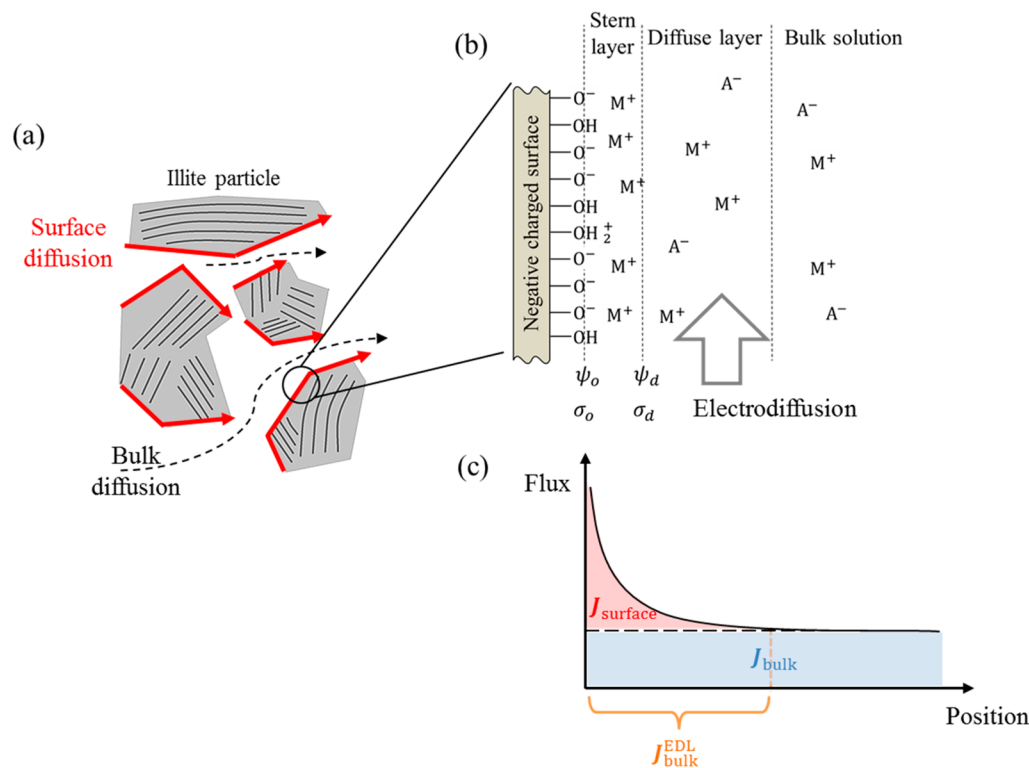


Figure 1. Sketch of surface diffusion and electrodiffusion in illite. (a) The clay particles and the diffusion pathway; the red lines show the pathway of surface diffusion. (b) The electrical double layer (EDL) near the charged clay surface. M⁺ denotes the cations and A⁻ the anions. (c) The corresponding flux composition within EDL.

factors.^{2,14,18} Our goals are (1) to reveal the mechanism of surface diffusion for simple positively charged tracers (like sodium ions) in compacted clays under a constant ion strength or under an ion strength gradient and (2) to quantitatively investigate under what conditions the cationic surface diffusion is significant.

2. CATION TRANSPORT WITHIN THE ELECTRICAL DOUBLE LAYER

Cationic Mobility. The surface of clays usually carries negative charges, which forms EDL structures when in contact with the electrolyte as shown in Figure 1b. The EDL structure generally includes two layers: the diffuse layer and the Stern layer. Because the local ionic mobility within pores depends on the distance away from clay surfaces,¹⁹ the pore size can affect the mean ionic mobility within pores. The previous molecular dynamic simulations^{20,21} suggested that the mean ionic mobility is about 60 to 90% of the mobility in the free water when the pore size is near 2 nm and the mean ionic mobility would tend to the mobility in free water with the increase of pore size. Because this study focuses on the clays whose mean pore size larger than 3 nm, we assume that the local mobility within pores is the same as that in free water. The relative error of calculated flux of sodium ions from this assumption should be less than 20% as the mean pore size is larger than 3 nm.

Surface Diffusion vs Electrodiffusion. The resolution of previous models is at continuum scale (i.e., centimeter or meter). Because the thickness of electrical double layer in clays is only several nanometers, the diffusion within EDL can be considered on the clay surface at continuum scale, as in the so-called “surface diffusion” shown in Figure 1a. In contrast, the pore-scale modeling can resolve the ion distribution within

EDL. Actually, the sorbed ions nearest to the mineral surface are mainly inner-sphere complexes, so the concept “surface diffusion” may cause misunderstanding at the pore scale. Hence, the concept of electrodiffusion is usually employed at the pore scale to describe sorbed-ion diffusion within EDL,^{18,22,23} shown in Figure 1b.

3. MODELING CATIONIC DIFFUSION AT THE PORE SCALE

The Nernst–Planck equations govern the evolutions of cationic electrodiffusion in porous media. By the treating of ions as point charges, the flux comes from pure diffusion and electromigration (or electrophoresis):²⁴

$$J_i^p = -D_{i,0} \nabla C_i^p - D_{i,0} \frac{z_i e C_i^p}{kT} \nabla \psi_i^p \quad (1)$$

$$\frac{\partial C_i^p}{\partial t} + \nabla \cdot J_i^p = 0 \quad (2)$$

where the J_i^p denotes the mass flux of the i^{th} ion species, $D_{i,0}$ is the diffusion coefficient of the i^{th} ion species in free water, C_i^p is the local concentration of the i^{th} ion species at pore scale, z_i is the i^{th} ion algebraic valence, e is the absolute charge of an electron, k is the Boltzmann constant, t is the time, and T is the absolute temperature. The superscript “P” means the corresponding term at pore scale. ψ_i^p denotes the local electrical potential related to the charged clay surface and to the local ion distribution, which is governed by the Poisson equation:

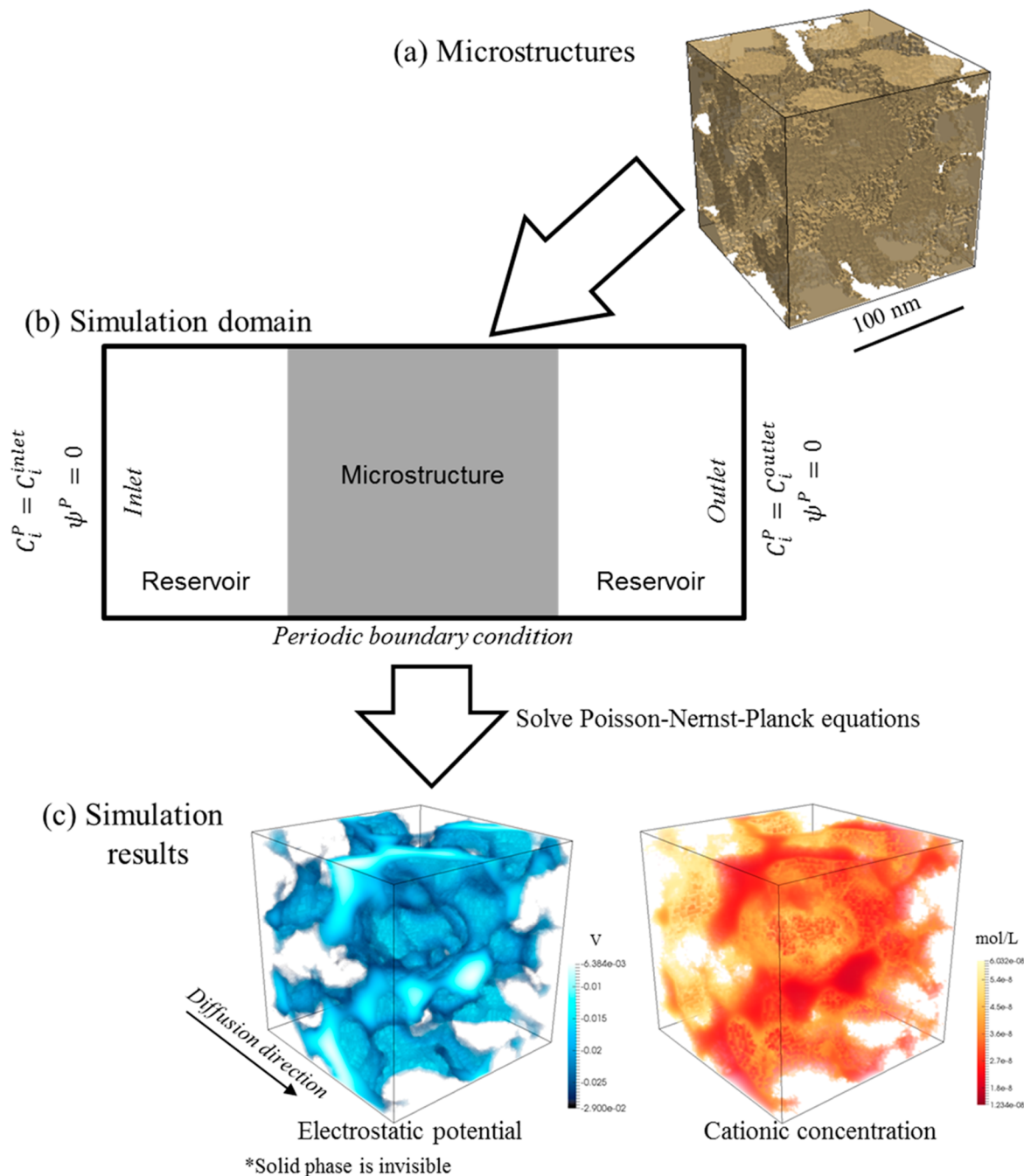


Figure 2. Schematic overview about this numerical framework to simulate ion diffusion in three-dimensional porous media. (a) The simulation is implemented in the realistic pore geometry extracted using the numerical generation method. (b) After solving of the coupled Poisson–Nernst–Planck equations in the simulation domain, (c) the local electrostatic potential and ionic concentration distributions within nanopores can be obtained as an example.

$$\nabla^2 \psi_i^P = -\frac{\rho_e^P}{\epsilon_r \epsilon_0} = -\sum_i \frac{N_A e z_i C_i^P}{\epsilon_r \epsilon_0} \quad (3)$$

where ρ_e^P is the net charge density, $\epsilon_r \epsilon_0$ is the dielectric constant of the pore solution, and N_A is the Avogadro’s number. Eqs 1 and 2 govern the ion transport process within EDL at pore-scale. Our model is based on the point charge assumption of ions; hence, our model is not valid for the electrolyte, which has high salinity (over 1 M) or exists in the oversized ions.²⁵

In this study, the coupled governing equations are directly solved in regenerated microstructures by our numerical framework based on the lattice Boltzmann method (LBM), whose detail is described in the Supporting Information. After the calculation, the local electrostatic potential and ionic concentration at pore scale can be determined shown in Figure 2. Based on the local information at pore scale, the statistical average flux of different species in geometry is estimated by using eq 1.²⁶ This numerical framework for ion transport in charged porous media has already been validated in our previous work,^{22,27} which indicates that the accuracy and robustness of our framework are suitable to capture

Table 1. Predictions of the Distribution Coefficient and the Relative Surface Diffusivity of Sodium Ions in Illite by Pore-Scale Modeling^a

ion salinity (mol/L)	distribution coefficient K_D (kg/m ³)		relative surface diffusivity μ_s			ratio of gradient $\frac{dC_s/dx}{dC/dx}$
	pore-scale modeling	experimental data ⁶	pore-scale modeling	fitting data in ref ²	ratio of concentration, C_s/C	
0.05	0.00407	–	0.14	0.07–0.8	43.19	3.78
0.1	0.00274	0.002	0.20		21.22	2.74
0.2	0.00153	–	0.31		10.25	2.00
0.5	0.000637	0.0005	0.51		3.83	1.25
1	0.000302	0.0002	0.69		1.79	0.79

^aOur pore-scale modeling also calculates the ratios of mean concentration and mean concentration gradient within the channel at the mid-section of the channel.

interactions between ions and charged surfaces. To simplify the simulation, we use the simple binary monovalent electrolyte solution (e.g., NaCl) as the electrolyte solution. The positive and neutral tracers (²²Na⁺ and HTO) are used to investigate the electrodiffusion within EDL in compacted clays. To refuse the influence of the tracer species on the chemical environment of the original pore solution, the tracer concentration should be low enough (less than 1×10^{-4} M). The pH value equals 7, and temperature T is equal to 298.15 K. The diffusivities for all species are assumed to be 1×10^{-10} m²/s at room temperature.

4. ELECTROKINETIC BOUNDARY CONDITIONS

Within EDL there are several important parameters: the surface charge density σ_0 or surface electrical potential ψ_0 and the diffuse layer charge density σ_d or ζ potential ψ_d . The surface charge density is the charge sites density on the solid clay surface, which corresponds to the cation exchange capacity (CEC in equivalents per kilogram) and to the total specific surface area (SSA in square meters per kilogram):

$$\sigma_0 = -\frac{eN_A \text{CEC}}{\text{SSA}} \quad (4)$$

The CEC changes with different clay minerals:⁶ ~ 1 equiv/kg for montmorillonite, ~ 0.1 equiv/kg for illite, and ~ 0.01 equiv/kg for kaolinite. The total surface area obtained by ethylene glycol monoethyl ether (EGME) method²⁸ was found to be ~ 700 m²/g for montmorillonite, ~ 100 m²/g for illite, and 50 m²/g for kaolinite. Hence, the surface charge density ranges from 0.01 C/m² to 0.2 C/m². The diffuse layer charge density σ_d and ζ potential ψ_d character the electrokinetic phenomena such as electroosmosis and electrophoresis. The ζ potential has the same order value for different clay minerals from -50 to -10 mV.²⁹ Because the pH and temperature are the constant throughout the simulated domain, the surface of clays is homogeneously charged. The surface potential or ζ potential depends on the ion strength,⁸ and therefore, the surface charge density σ_0 is adopted as the boundary condition for the Poisson equation in this study to describe the electrokinetic effects on cationic electrodiffusion.

5. VALIDATION OF THE PORE-SCALE SIMULATION

In this section, this pore-scale modeling is validated with experimental data and previous reported models by predicting the distribution coefficient K_D and the relative surface diffusivity μ_s of sodium ions. To simplify the simulation, a three-dimensional straight nanochannel is considered as the simulation domain. The detail of simulation domain and

corresponding boundary conditions is shown in Figure S1. The bulk pore solution is set as 0.05, 0.1, 0.2, 0.5, and 1.0 M NaCl, respectively. The tracer's concentration is $C_{\text{tracer}}^{\text{inlet}} = 2.0 \times 10^{-5}$ M at the inlet and $C_{\text{tracer}}^{\text{outlet}} = 1.0 \times 10^{-5}$ M at the outlet. To be consistent with Glaus' experiment for sodium ion in illite,⁶ the pore size h equals 3.5 nm, and the surface charge density is set as -0.19 C/m². The other parameters are the same as those in ref 27.

It is necessary to clarify how to calculate the flux of surface diffusion in this work. In fact, there are two definitions of surface diffusion: the surface diffusion is the diffusion of cations in EDL along the clay surface⁵ or the surface diffusion is the excess mobility of the cation due to the excess of sorbed cations within EDL.³⁰ At the continuum scale, the total flux of sorbed cation in clays is considered as the sum of flux from the normal diffusion in pores J_{bulk} and that from the surface diffusion J_{surface} as:²

$$J = J_{\text{bulk}} + J_{\text{surface}} = -D_{e, \text{uncharge}} \frac{dC}{dx} - D_s \frac{dC_s}{dx} = -D_{e, \text{cation}} \frac{dC}{dx} \quad (5)$$

where $D_{e, \text{uncharge}}$ is the effective diffusivity of uncharged species in clays, D_s is the surface diffusivity, C is the concentration in bulk solution, C_s is the sorbed cation concentration on the surface, and $D_{e, \text{cation}}$ is the effective diffusivity of cations in clays. The relative surface diffusivity is defined as:

$$\mu_s = D_s/D_0 \quad (6)$$

Therefore, in previous one-dimensional modeling,^{2,14} the cationic tracer's effective diffusivity $D_{e, \text{cation}}$ in eq 4 is usually described as:

$$D_{e, \text{cation}} = \frac{\theta}{\tau} D_0 + \frac{\rho_{\text{bd}} K_D \mu_s}{\tau} D_0 \quad (7)$$

where θ is the porosity of clay, τ is tortuosity, and ρ_{bd} is the dry bulk density of clay. The distribution coefficient K_D is calculated by:¹⁴

$$K_D = \frac{\bar{C}_s^{\text{P}} - \bar{C}^{\text{P}}}{\bar{C}^{\text{P}} \rho_{\text{bd}}} \theta \quad (8)$$

where \bar{C}_s^{P} is the mean concentration of cations within pores, and \bar{C}^{P} is the mean concentration of uncharged species in the same condition as cations. J_{bulk} of the sorbed cations is obtained by using $D_{e, \text{uncharge}}$, which is determined by the uncharged species such as tritium water (HTO). The total flux J equals to the sum of J_{surface} and J_{bulk} . Note that the neutral

species is accessible into EDL, and the cationic flux within EDL J_{EDL} actually combines some from J_{bulk} with all from $J_{surface}$ shown in Figure 1:

$$J_{EDL} = J_{surface} + J_{bulk}^{EDL} \quad (9)$$

with J_{bulk}^{EDL} the flux of neutral species within EDL. It means that the flux from surface diffusion should be the excess flux of the sorbed cations due to the excess of cations within EDL.

The predicted K_D of sodium ions in illite by our modeling is consistent with the experimental data at similar conditions,⁶ and the range of relative surface diffusivity matches up with the fitting values in previous reported modeling² listed in Table 1. Besides, our modeling shows that the relative surface diffusivity decreases when the ion salinity is reduced. Note that the constant diffusivity is used in our modeling. This reveals that the observed slower surface diffusivity may not describe the real local ionic mobility near the clay surface.

To obtain the effective diffusivity of cations in eqs 6 from eqs 4, the previous generalized Fick's law employed the assumption:^{2,14,31}

$$\frac{dC_s}{dC} = \frac{dC_s/dx}{dC/dx} = \frac{C_s}{C} \quad (10)$$

This assumption suggested that the ratio of mean concentration gradient within pores along transport direction between sorbed cations and nonsorbed cations should equal the ratio of corresponding mean concentration within pores. Table 1 shows the ratios of mean concentration gradient and mean concentration within pores calculated by our model, which found that dC_s/dC is much lower than C_s/C in the low-salinity solution. The thickness of EDL increases as the ion salinity becomes lower.¹⁴ For the low ion salinity, the strong overlapping EDL reorganizes the ion distributions and the classical models breaks down.³² For instance, the classical Gouy–Chapman model will underestimate the concentration of counterions than the direct simulation as EDL strongly overlaps.³³

6. RESULTS AND DISCUSSION

We investigate the influences from both topological properties (such as surface area and porosity) and surface electrokinetic properties (such as surface charge density or ion strength) on tracer's electrodiffusion. To character the importance of cationic electrodiffusion (or surface diffusion at the macro scale), we define the ratio of the surface electrodiffusion, φ , of sodium ions as:

$$\varphi = J_{electro}/J = J_{electro}/(J_{electro} + J_{bulk}) \quad (11)$$

where J denotes the total flux of monovalence tracer and $J_{electro}$ the excess flux of the sorbed cationic tracer at the pore scale, which equals $J_{surface}$ at the macroscale. The J_{bulk} is calculated by the neutral tracer HTO in the same conditions as the sodium ions. This ratio φ characters the contribution from cationic electrodiffusion to the total flux at pore scale. Our pore-scale simulation can obtain the J and $J_{electro}$, then we use eq 10 to calculate the ratio of electrodiffusion. However, at macroscale or in experiment, it is difficult to separate the contributions from electrodiffusion and bulk diffusion of sodium ions. The ratio of electrodiffusion φ in experiment is obtained by using the effective diffusivities of HTO and sodium ions:

$$\varphi = \frac{D_{e,Na^+} - D_{0,Na^+}D_{e,HTO}/D_{0,HTO}}{D_{e,Na^+}} \quad (12)$$

where D_{e,Na^+} and $D_{e,HTO}$ are effective diffusivities of sodium and HTO in clays measured by the through-diffusion test. D_{0,Na^+} and $D_{0,HTO}$ are the sodium and HTO diffusivity in free water. If $\varphi > 0.7$, the electrodiffusion or the surface diffusion is considered as the dominated transport process in compacted clays in this study; while if $\varphi < 0.3$, it is unimportant. In charged porous media, the normalized volume charge density ρ_e^* (C/m^3) is defined as

$$\rho_e^* = -\frac{\sigma_0 S}{\theta e N_A I_s} = \frac{CEC \rho_{bd}}{\theta I_s} \quad (13)$$

where S (square meter per cubic meter) denotes the surface area per unit volume, and θ the porosity. The ion strength I_s depends on the bulk concentration C_i as $I_s = 0.5 \sum z_i^2 C_i$, and a lower ion strength leads to a larger thickness of EDL. In the previous studies,^{11,34} the normalized volume charge density ρ_e^* was used as an index to character the strength of EDL effects. Based on the reported modeling using the Donnan theory,¹¹ eq 10 changes to:

$$\varphi = 1 + \frac{\rho_e^*}{2} - \sqrt{\left(\frac{\rho_e^*}{2}\right)^2 + 1} \quad (14)$$

The cationic electrodiffusion in eq 1 consists of the pure diffusion term, $D_{i,0} \nabla C_i^P$, and the electrophoretic term, $D_{i,0} z_i e C_i^P \nabla \psi^P / kT$. There is, however, no agreement about the contribution from each term to the total electrodiffusion. Revil et al.³⁵ suggested that it is a pure electromigration process due to the membrane potential in clays, yet Oscarson⁵ proposed that it is pure diffusion process caused by the increase of the concentration gradient. Hence, to characterize the importance of electromigration (or electrophoresis) process in clays, another ratio between the total cationic tracer's flux from the electro-potential gradient and from the concentration gradient Ξ is defined as:

$$\Xi = \left| \frac{\iint -D_{i,0} z_i e C_i^P \nabla \psi^P ds}{kT \iint -D_{i,0} \nabla C_i^P ds} \right| \quad (15)$$

where $\iint [\cdot] ds$ is the surface integral on cross-sections normal to the transport direction. When $\Xi \geq 0.1$, it means that the cation flux from electromigration (or electrophoresis) by the inner electric field (or membrane potential) along transport direction in clays cannot be ignored, but as $\Xi < 0.1$, the electrophoretic process has little contribution to the total flux of cation and is negligible.

In this study, two situations, in which cationic tracer diffuses, are considered: the ionic strength is constant throughout the simulated domain or a linear ionic strength gradient along the ion transport direction. A constant ionic strength is normally adopted in experimental measurements.^{1,6} Because the ion strength is constant, the local electrical distribution can be calculated by the efficient Poisson–Boltzmann model.¹¹ For the second situation, a linear ionic strength is applied along the transport direction, which was reported by Glaus et al.³⁶ In this situation, the local electrical distribution is solved by coupled Poisson–Nernst–Planck model.

Tracer Diffusion under a Constant Ion Strength. The tracer's flux is calculated in the microstructures of compacted

Table 2. Total Flux of Sodium Tracer and HTO in Clays and the Corresponding Ratio of Electrodiffusion ϕ Calculated by Our Pore-Scale Modeling at a Constant Ion Strength^a

porosity θ	surface charge density σ_0 (C/m ²)	ion strength I_s (mol/L)	surface area per unit volume S (nm ⁻¹)	flux J ($\times 10^{-9}$ mol/m ² /s)		ρ^*	ϕ
				Na ⁺	HTO		
0.3	-0.002	0.0005	0.251	9.382	0.684	34.71	0.927
0.3	-0.001	0.001	0.251	5.115	0.684	8.68	0.866
0.3	-0.0004	0.001	0.251	2.749	0.684	3.47	0.751
0.3	-0.0002	0.001	0.251	1.665	0.684	1.74	0.589
0.4	-0.1	0.01	0.087	3.650	0.861	22.45	0.764
0.4	-0.01	0.01	0.087	1.785	0.861	2.25	0.518
0.4	-0.004	0.001	0.087	3.522	0.861	8.98	0.756
0.4	-0.001	0.01	0.087	0.964	0.861	0.22	0.107
0.5	-0.002	0.0005	0.281	8.516	1.700	23.34	0.800
0.5	-0.001	0.0001	0.281	13.307	1.700	58.35	0.872
0.5	-0.001	0.0002	0.281	9.965	1.700	29.17	0.829
0.5	-0.001	0.001	0.281	5.295	1.700	5.83	0.679
0.5	-0.0004	0.0001	0.281	9.832	1.700	23.34	0.827
0.5	-0.0004	0.001	0.281	3.480	1.700	2.33	0.512
0.5	-0.0002	0.001	0.281	2.594	1.700	1.17	0.345
0.6	-0.1	0.01	0.077	3.819	1.512	13.33	0.604
0.6	-0.01	0.01	0.077	2.294	1.512	1.33	0.341
0.6	-0.004	0.001	0.077	3.777	1.512	5.33	0.600
0.7	-0.002	0.0005	0.251	8.635	2.660	14.87	0.692
0.7	-0.001	0.0001	0.251	13.554	2.660	37.19	0.804
0.7	-0.001	0.001	0.251	5.574	2.660	3.72	0.523
0.7	-0.0004	0.0001	0.251	10.135	2.660	14.87	0.738
0.7	-0.0004	0.001	0.251	4.063	2.660	1.49	0.345
0.7	-0.0002	0.001	0.251	3.378	2.660	0.74	0.213

^aIn our simulation, the normalized volume charge density ρ^* is calculated by eq 12; $J_{\text{electro}} = J_{\text{Na}^+} - J_{\text{HTO}}$.

clays by the present pore-scale numerical framework. To directly probe the nature texture of clays at nanoscale is high-cost and time-consuming;³⁵ therefore, the pore structures of clay in this study is generated by the numerical reconstructed techniques.^{37,38} In this study, we employ the QSGS algorithm to restructure the porous microstructures of clays³⁹ and the properties at the REV scale (such as porosity, bulk density, and mean particle size) of regenerated microstructure can be controlled by this method. The clay is fully saturated, and the solid phase is not diffusive. A 192 nm \times 192 nm \times 192 nm cubic porous clay with two transition regions is used for simulation, as shown in Figure S2, which is large enough to satisfy the REV requirement for typical compacted clays. To resolve the electrical double layer structure, the resolution of our simulation is 0.75 nm. The other parameters are the same as mentioned before. The pore-scale modeling can resolve the local pore morphology of clays, and the local ion distributions are shown in Figure 2c. Due to the inhomogeneous local electrical potential distribution, the concentration distributions at pore scale in compacted clays are also inhomogeneous. We analyze the influences from four parameters on the total sodium tracer's flux quantitatively: surface charge density σ_0 , ion strength I_s , porosity, and surface area per unit volume S .

To clarify the interrelated influence from both EDL and topology on cationic electrodiffusion, a series of microstructures of compacted clays are generated in which the porosity changes from 0.3 to 0.7. In our simulation, the bulk concentration of ²³NaCl ranges from 10⁻² to 10⁻⁴ mol/L so that the corresponding EDL thickness changes from 15 to 150 nm.⁴⁰ The surface charge density changes from -0.0002 to -0.1 C/m². Our simulation results tabulated in Table 2 show

that the ²²Na⁺ tracer's flux increases as the ion strength decrease but the HTO tracer's flux is almost constant, which is consistent with the reported experiment results.^{1,6}

Figure 3 indicates that the ratio of electrodiffusion with respect to normalized volume charge density is in a nonlinear relationship. The ratio ϕ increases as ρ^* increases and trends

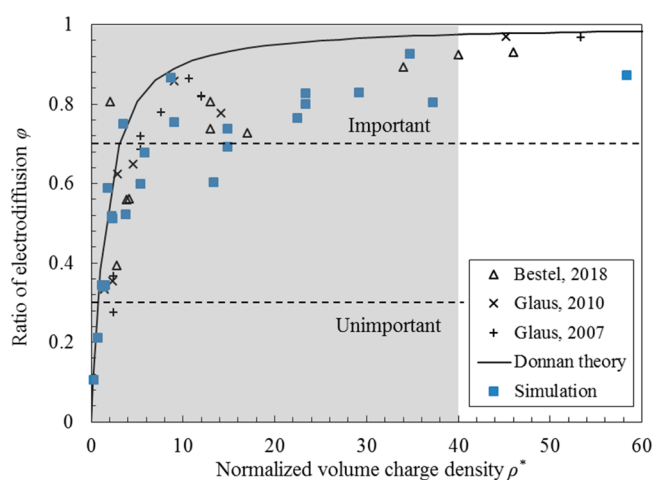


Figure 3. Ratio of electrodiffusion ϕ with respect to the normalized volume charge density ρ^* . The blue square is our simulation results, and the black points are reported experiment data in compacted montmorillonite, illite, and kaolinite^{6,41,42} (the values are tabulated in Table S1). The black line is predicted by eq 13 based on the Donnan theory. The shaded area is the region where our pore-scale modeling is valid.

Table 3. Ion Strength Gradient Applied in a Two-Dimensional Channel and Cationic Tracer Total Fluxes from Pure Diffusion Terms ($-D_i \nabla C_i$) and Electromigration Term ($-D_i z_i e C_i \nabla \psi / kT$) on the Cross-Section^a

$\Delta C/\bar{C}$	concentration gradient of cation tracer (mol/m ⁴)	flux from pure diffusion ($\times 10^{-7}$ mol/m ² /s)	flux from electromigration ($\times 10^{-7}$ mol/m ² /s)	sum of flux ($\times 10^{-7}$ mol/m ² /s)	φ	Ξ
-1.6	0.28	-1.40	3.07	1.67	0.55	2.19
-0.8	-0.05	0.23	1.37	1.60	0.53	5.99
-0.4	-0.18	0.92	0.67	1.59	0.52	0.74
0	-0.32	1.58	0.00	1.58	0.52	0.00
0.4	-0.45	2.27	-0.68	1.59	0.52	0.30
0.8	-0.61	3.03	-1.42	1.61	0.53	0.47
1.6	-1.01	5.02	-3.34	1.68	0.55	0.67

^aThe surface charge density is -0.01 C/m². The average concentration $\bar{C} = (C_0^{\text{inlet}} + C_0^{\text{outlet}})/2$ equals 0.01 mol/L.

toward one. Because ρ^* is less than 1, φ is less than 0.3, which means that the electrodiffusion of cation is negligible. The electrodiffusion (or the surface diffusion at the REV scale) becomes the dominant diffusion process for cations when ρ^* reaches 20. For instance, as the bulk concentration equals to 0.1 M, the experiment data reported by Glaus⁶ indicated that ρ^* equals 2.3 in kaolinite with the low surface charge and φ equals 0.36. However, for the high surface charge case in the same conditions, $\varphi = 0.78$ when $\rho^* = 14.1$ in illite and $\varphi = 0.97$ when $\rho^* = 45.2$ in montmorillonite. Our simulation in Table 2 shows that φ ranges from 0.345 to 0.872 when ρ^* increases from 1.17 to 58.35, which quantitatively agrees with the experimental data. The Donnan theory predicts larger values than experiment data when normalized volume charge density is less than 40 (shaded area in Figure 3), where the surface diffusion gradually changes from unimportant to important. When normalized volume charge density is larger than 40 (unshaded area in Figure 3), the clay usually has narrow nanopores, and the steric effect becomes important, which breaks the assumption of our simulation.

For the constant-ion-strength case, the thickness of EDL is changeless. The inner electrical field along the diffusion direction has little impact on ion transport. The contribution ratio of flux from the electromigration to that from the concentration gradient is less than 0.01 ($\Xi < 0.01$) calculated by our pore-scale modeling. It means that the cation flux from electromigration process is negligible. Therefore, the flux of positive monovalent tracer comes mainly from the pure diffusion process for the constant ion strength case. These results reveal that the cationic diffusion in the less-charged clays is mainly affected by the connectivity and tortuosity, but in clays with a high surface area or surface charge density, the electrodiffusion is the dominant process and the influence from EDL is significant. These are also consistent with the previous experimental measurements^{6,43} where for the montmorillonite, the surface charge was usually high enough to make the electrodiffusion usually important. However, the electrodiffusion may be not so important in kaolinite due to its low CEC value and the influence from topology on diffusion becomes relatively significant.

Tracer Diffusion under an Ion Strength Gradient. In this situation, the numerical instability significantly increases, and the mesh should be refined at least 8 more times than the previous case, which causes the computing efforts to exponentially increase. Therefore, the two-dimensional nano-channel is used as the geometry of simulation. The simulation domain and corresponding boundary conditions are shown in Figure S3. The width of the channel is 8 nm, and the surface charge density is -0.01 C/m². To generate a constant ion

strength gradient in the simulated domain, the normalized concentration differences $\Delta C/\bar{C} = (C_0^{\text{outlet}} - C_0^{\text{inlet}})/\bar{C}$ at boundaries are set as $-1.6, -0.8, -0.4, 0, 0.4, 0.8,$ and 1.6 , respectively, where the average concentration $\bar{C} = (C_0^{\text{inlet}} + C_0^{\text{outlet}})/2$ is kept as 0.01 mol/L. The tracer's concentration is $C_{\text{tracer}}^{\text{inlet}} = 2.0 \times 10^{-8}$ M at the inlet and $C_{\text{tracer}}^{\text{outlet}} = 1.0 \times 10^{-8}$ M at the outlet. The other parameters are the same as mentioned before. The cationic tracer's fluxes from the pure diffusion and the electromigration terms are calculated in these situations listed in Table 3.

As shown in Table 3, the flux from electromigration can be ignored when the ion strength is constant ($\Delta C/\bar{C} = 0$). However, if apply an ion strength gradient $\Delta C/\bar{C} \neq 0$, the simulation shows that the total flux is from both pure diffusion and electromigration, but the total flux is nearly the same for all cases. Actually, the changes of flux caused by the pure diffusion finally offset by the electromigration, and this balance therefore causes a little change of total flux shown in Figure 4. For instance, the ion strength increases along the tracer transport direction because $\Delta C/\bar{C}$ equals to 0.8. Because the lower ion strength side has lower mean electrical potential and can adsorb more sodium tracer ions,⁴⁴ the direction of flux from the electromigration term is opposite to the flux from pure diffusion term, as shown in Figure 4a,d. Note that the ratio Ξ reflects the importance of electromigration terms of the sodium ions. Hence, the electromigration process is significant as the absolute value of $\Delta C/\bar{C}$ increases. However, the previous reported models^{11,14} ignored the ion motion by the electrophoresis, which only considers the ion transport driven by the concentration gradient. Our pore-scale modeling shows that the contribution from electromigration should be respected because its non-negligible role to balance the total flux as the inner membrane electrical field exists in clays and the flux of cationic tracer in this situation can be predicted from the situation with the constant ion strength situation. Table S2 also indicates that the ratio Ξ follows the same trend of ratio φ . The ratio Ξ is larger in the lower-salinity solution or in clays with higher surface charge density as $\Delta C/\bar{C} \neq 0$.

Environmental Implications. The EDL overlap within nanopores of compacted clays may magnify the impact of this two-way coupling between the electrokinetic effect and the cationic diffusion process. The continuum-scale models fitting with experimental results are limited on understanding this coupled process in compacted clay. The proposed pore-scale modeling has important implications for the quantification of simple cationic transport in compacted clays in the background of the geosphere transport of radioactive material, which is also helpful for future experimental design. In particular, the classical Gouy–Chapman model falls as EDL overlaps.³³ To

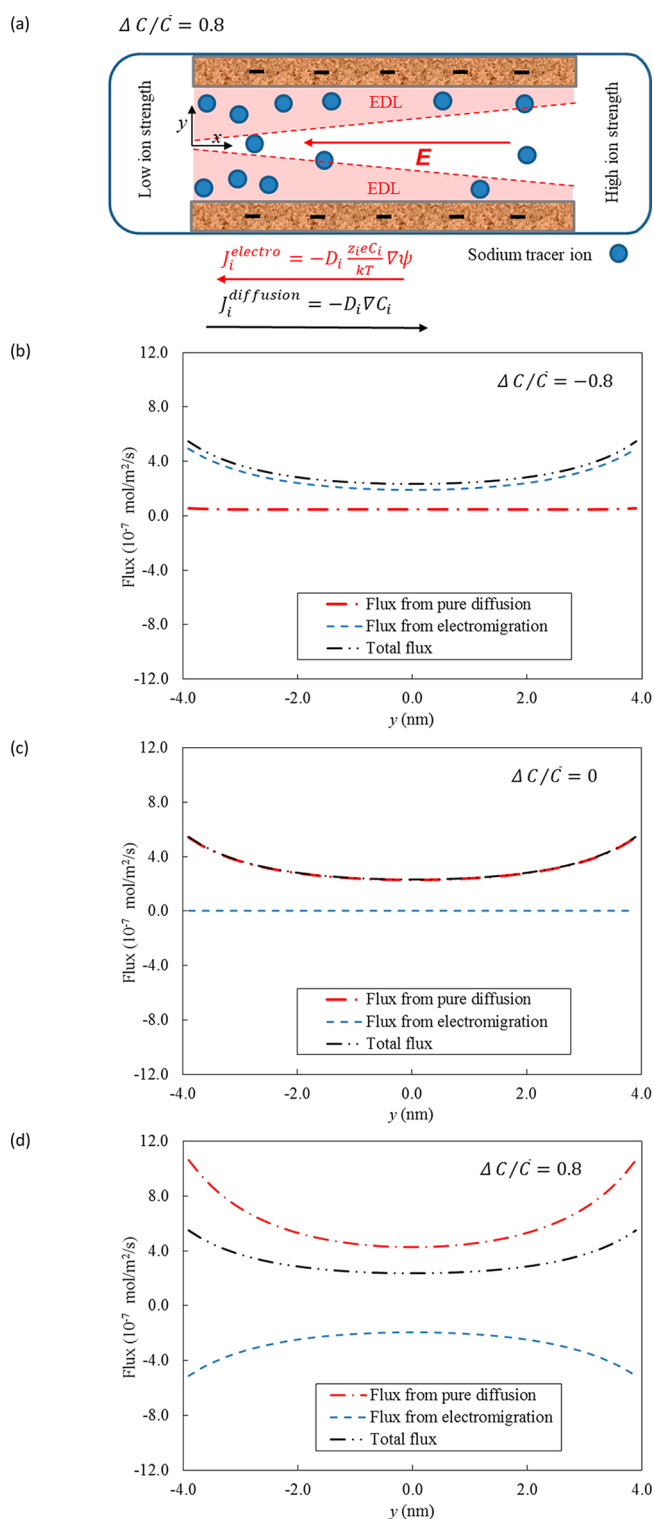


Figure 4. Sketch of sodium tracer ion's electrodiffusion as an ion strength gradient applied in panel a. The red dashed lines represent the boundary of EDL. The side with the low ion strength has large EDL thickness, so it can adsorb more sodium tracer ions. The red arrow denotes the inner electrical field E . The directions of flux from pure diffusion (black) and electromigration (blue) are different. (b–d) The flux distributions from pure diffusion (red line), electromigration (blue line), and total flux (black line) terms along the x direction on the cross-section of nanochannel for different ion strength gradients: (b) $\Delta C/\bar{C} = -0.8$, (c) $\Delta C/\bar{C} = 0$, and (d) $\Delta C/\bar{C} = 0.8$.

directly solve coupled Poisson–Nernst–Planck equations at the pore scale can overcome this shortage and clarify effects from different physical or chemical factors. Simulations in this work were run to hours when steady-state conditions were reached, which is time-saving and cheaper to implement compared with experiment. The present study quantitatively characterizes the contribution from surface diffusion in compacted clay under different situations. The significant impact of the parameter of normalized volume charge density on cationic surface diffusion is consistent with the previous studies.^{8,11,34} Actually, the linear change of ionic strength along the diffusion direction can occur in the field⁹ or in laboratory conditions,³⁶ while most of the experiments or models are implemented using the constant ionic strength assumption. However, as an ionic strength gradient exists, the membrane potential has an important impact on electromigration terms in eq 1, which should be respected in future studies.

■ ASSOCIATED CONTENT

📄 Supporting Information

The Supporting Information is available free of charge on the ACS Publications website at DOI: 10.1021/acs.est.8b05755.

Details on the pore-scale numerical framework; figures showing the simulated domains for each case; tables showing the reported experimental data and simulation results as an ion strength gradient is applied (PDF)

■ AUTHOR INFORMATION

Corresponding Author

*E-mail: mrwang@tsinghua.edu.cn. Phone: 86-10-627-87498.

ORCID

Moran Wang: 0000-0002-0112-5150

Notes

The authors declare no competing financial interest.

■ ACKNOWLEDGMENTS

This work is financially supported by the NSF of China (grant no. 51766107). Y.Y. thanks the helpful discussion with Ravi A. Patel, Philipp Krejci, and Dr. Georg Kosakowski in Paul Scherrer Institute, Switzerland.

■ REFERENCES

- (1) Tachi, Y.; Yotsuji, K. Diffusion and sorption of Cs^+ , Na^+ , I^- and HTO in compacted sodium montmorillonite as a function of porewater salinity: Integrated sorption and diffusion model. *Geochim. Cosmochim. Acta* **2014**, *132*, 75–93.
- (2) Gimmi, T.; Kosakowski, G. How mobile are sorbed cations in clays and clay rocks? *Environ. Sci. Technol.* **2011**, *45* (4), 1443–9.
- (3) Cho, W. J.; Oscarson, D. W.; Gray, M. N.; Cheung, S. C. H. Influence of Diffusant Concentration on Diffusion Coefficients in Clay. *Radiochim. Acta* **1993**, *60*, 159.
- (4) Cormenzana, J. L.; García-Gutiérrez, M.; Missana, T.; Junghanns, Á. Simultaneous estimation of effective and apparent diffusion coefficients in compacted bentonite. *J. Contam. Hydrol.* **2003**, *61* (1–4), 63–72.
- (5) Oscarson, D. W. Surface diffusion: Is it an important transport mechanism in compacted clays? *Clays Clay Miner.* **1994**, *42* (5), 534–543.
- (6) Glaus, M. A.; Frick, S.; Rossé, R.; Loon, L. R. V. Comparative study of tracer diffusion of HTO, $^{22}\text{Na}^+$ and $^{36}\text{Cl}^-$ in compacted kaolinite, Illite and montmorillonite. *Geochim. Cosmochim. Acta* **2010**, *74* (7), 1999–2010.

- (7) Glaus, M. A.; Aertsens, M.; Appelo, C. A. J.; Kupcik, T.; Maes, N.; Van Laer, L.; Van Loon, L. R. Cation diffusion in the electrical double layer enhances the mass transfer rates for Sr²⁺, Co²⁺ and Zn²⁺ in compacted Illite. *Geochim. Cosmochim. Acta* **2015**, *165*, 376–388.
- (8) Leroy, P.; Revil, A.; Coelho, D. Diffusion of ionic species in bentonite. *J. Colloid Interface Sci.* **2006**, *296* (1), 248–55.
- (9) Jougnot, D.; Revil, A.; Leroy, P. Diffusion of ionic tracers in the Callovo-Oxfordian clay-rock using the Donnan equilibrium model and the formation factor. *Geochim. Cosmochim. Acta* **2009**, *73* (10), 2712–2726.
- (10) Birgersson, M.; Karnland, O. Ion equilibrium between montmorillonite interlayer space and an external solution—Consequences for diffusional transport. *Geochim. Cosmochim. Acta* **2009**, *73* (7), 1908–1923.
- (11) Birgersson, M. A general framework for ion equilibrium calculations in compacted bentonite. *Geochim. Cosmochim. Acta* **2017**, *200*, 186–200.
- (12) Appelo, C. A. J.; Wersin, P. Multicomponent Diffusion Modeling in Clay Systems with Application to the Diffusion of Tritium, Iodide, and Sodium in Opalinus Clay. *Environ. Sci. Technol.* **2007**, *41* (14), 5002–5007.
- (13) Bourg, I. C.; Sposito, G.; Bourg, A. Tracer diffusion in compacted, water-saturated bentonite. *Clays Clay Miner.* **2006**, *54* (3), 363–374.
- (14) Tinnacher, R. M.; Holmboe, M.; Tournassat, C.; Bourg, I. C.; Davis, J. A. Ion adsorption and diffusion in smectite: Molecular, pore, and continuum scale views. *Geochim. Cosmochim. Acta* **2016**, *177*, 130–149.
- (15) Tournassat, C.; Steefel, C. I. Ionic Transport in Nano-Porous Clays with Consideration of Electrostatic Effects. *Rev. Mineral. Geochem.* **2015**, *80* (1), 287–329.
- (16) Appelo, C. A. J.; Van Loon, L. R.; Wersin, P. Multicomponent diffusion of a suite of tracers (HTO, Cl, Br, I, Na, Sr, Cs) in a single sample of Opalinus Clay. *Geochim. Cosmochim. Acta* **2010**, *74* (4), 1201–1219.
- (17) Messinger, R. J.; Squires, T. M. Suppression of electro-osmotic flow by surface roughness. *Phys. Rev. Lett.* **2010**, *105* (14), 144503.
- (18) Yang, Y.; Wang, M. Pore-scale study of thermal effects on ion diffusion in clay with inhomogeneous surface charge. *J. Colloid Interface Sci.* **2018**, *514*, 443–451.
- (19) Ichikawa, Y.; Kawamura, K.; Fujii, N.; Nattavut, T. Molecular dynamics and multiscale homogenization analysis of seepage/diffusion problem in bentonite clay. *International Journal for Numerical Methods in Engineering* **2002**, *54* (12), 1717–1749.
- (20) Kosakowski, G.; Churakov, S. V.; Thoenen, T. Diffusion of Na and Cs in montmorillonite. *Clays Clay Miner.* **2008**, *56* (2), 190–206.
- (21) Holmboe, M.; Bourg, I. C. Molecular Dynamics Simulations of Water and Sodium Diffusion in Smectite Interlayer Nanopores as a Function of Pore Size and Temperature. *J. Phys. Chem. C* **2014**, *118* (2), 1001–1013.
- (22) Rubinstein, S. M.; Manukyan, G.; Staicu, A.; Rubinstein, I.; Zaltzman, B.; Lammertink, R. G. H.; Mugele, F.; Wessling, M. Direct Observation of a Nonequilibrium Electro-Osmotic Instability. *Phys. Rev. Lett.* **2008**, *101* (23), 236101.
- (23) Boda, D.; Gillespie, D. Steady-State Electrodiffusion from the Nernst-Planck Equation Coupled to Local Equilibrium Monte Carlo Simulations. *J. Chem. Theory Comput.* **2012**, *8* (3), 824–9.
- (24) Probst, R. F. *Physicochemical hydrodynamics: an introduction*; John Wiley & Sons: Hoboken, NJ, 2005.
- (25) Wang, M.; Liu, J.; Chen, S. Electric potential distribution in nanoscale electroosmosis: from molecules to continuum. *Mol. Simul.* **2008**, *34* (5), 509–514.
- (26) Yang, Y.; Patel, R. A.; Churakov, S. V.; Prasianakis, N. I.; Kosakowski, G.; Wang, M. Multiscale modeling of ion diffusion in cement paste: electrical double layer effects. *Cem. Concr. Compos.* **2019**, *96*, 55–65.
- (27) Tian, H.; Zhang, L.; Wang, M. Applicability of Donnan equilibrium theory at nanochannel-reservoir interfaces. *J. Colloid Interface Sci.* **2015**, *452*, 78–88.
- (28) González Sánchez, F.; Van Loon, L. R.; Gimmi, T.; Jakob, A.; Glaus, M. A.; Diamond, L. W. Self-diffusion of water and its dependence on temperature and ionic strength in highly compacted montmorillonite, Illite and kaolinite. *Appl. Geochem.* **2008**, *23* (12), 3840–3851.
- (29) Chorom, M.; Rengasamy, P. Dispersion and zeta potential of pure clays as related to net particle charge under varying pH, electrolyte concentration and cation type. *Eur. J. Soil Sci.* **1995**, *46* (4), 657–665.
- (30) Shackelford, C. D.; Moore, S. M. Fickian diffusion of radionuclides for engineered containment barriers: Diffusion coefficients, porosities, and complicating issues. *Eng. Geol.* **2013**, *152* (1), 133–147.
- (31) Bourg, I. C.; Sposito, G.; Bourg, A. C. M. Modeling Cation Diffusion in Compacted Water-Saturated Sodium Bentonite at Low Ionic Strength. *Environ. Sci. Technol.* **2007**, *41* (23), 8118–8122.
- (32) Miller, A. W.; Wang, Y. Radionuclide interaction with clays in dilute and heavily compacted systems: a critical review. *Environ. Sci. Technol.* **2012**, *46* (4), 1981–94.
- (33) Wang, M.; Revil, A. Electrochemical charge of silica surfaces at high ionic strength in narrow channels. *J. Colloid Interface Sci.* **2010**, *343* (1), 381–6.
- (34) Gimmi, T.; Alt-Epping, P. Simulating Donnan equilibria based on the Nernst-Planck equation. *Geochim. Cosmochim. Acta* **2018**, *232*, 1–13.
- (35) Revil, A.; Pezard, P. A.; Glover, P. W. J. Streaming potential in porous media: 1. Theory of the zeta potential. *Journal of Geophysical Research: Solid Earth* **1999**, *104* (B9), 20021–20031.
- (36) Glaus, M. A.; Birgersson, M.; Karnland, O.; Van Loon, L. R. Seeming steady-state uphill diffusion of ²²Na⁺ in compacted montmorillonite. *Environ. Sci. Technol.* **2013**, *47* (20), 11522–7.
- (37) Tyagi, M.; Gimmi, T.; Churakov, S. V. Multi-scale microstructure generation strategy for up-scaling transport in clays. *Adv. Water Resour.* **2013**, *59*, 181–195.
- (38) Wang, M.; Chen, S. Electroosmosis in homogeneously charged micro- and nanoscale random porous media. *J. Colloid Interface Sci.* **2007**, *314* (1), 264–73.
- (39) Wang, M.; Wang, J.; Pan, N.; Chen, S. Mesoscopic predictions of the effective thermal conductivity for microscale random porous media. *Phys. Rev. E* **2007**, *75* (3), 036702.
- (40) Zhang, L.; Wang, M. Electro-osmosis in inhomogeneously charged microporous media by pore-scale modeling. *J. Colloid Interface Sci.* **2017**, *486*, 219–231.
- (41) Bestel, M.; Glaus, M. A.; Frick, S.; Gimmi, T.; Juranyi, F.; Van Loon, L. R.; Diamond, L. W. Combined tracer through-diffusion of HTO and ²²Na through Na-montmorillonite with different bulk dry densities. *Appl. Geochem.* **2018**, *93*, 158–166.
- (42) Glaus, M. A.; Baeyens, B.; Bradbury, M. H.; Jakob, A.; Van Loon, L. R.; Yaroshchuk, A. Diffusion of ²²Na and ⁸⁵Sr in Montmorillonite: Evidence of Interlayer Diffusion Being the Dominant Pathway at High Compaction. *Environ. Sci. Technol.* **2007**, *41* (2), 478–485.
- (43) Molera, M.; Eriksen, T. Diffusion of ²²Na⁺, ⁸⁵Sr²⁺, ¹³⁴Cs⁺ and ⁵⁷Co²⁺ in bentonite clay compacted to different densities: experiments and modeling. *Radiochim. Acta* **2002**, *90* (9-11), 753–760.
- (44) Donnan, F. G. The Theory of Membrane Equilibria. *Chem. Rev.* **1924**, *1* (1), 73–90.